Towards a Universal Multiresolution-Based Perceptual Model

Lahouari Ghouti and Ahmed Bouridane

Abstract— **Following a recently introduced perceptual model for balanced multiwavelets, we outline, in this paper, an extension of our previous work and propose a new perceptual model for scalar wavelets. The proposed model is derived using multiresolution domain extensions of our previous scheme. Unlike existing models, the proposed one depends only on the image activity and not the filter sets used by the transform. The perceptual redundancy, present in the image, is efficiently quantified through a just-noticeable distortion (JND) profile. In this model, a visibility threshold of distortion is assigned to each wavelet subband coefficient. Therefore, perceptually insignificant subband components can be clearly discriminated from perceptually significant ones. For instance, this discrimination can be constructively used to achieve the imperceptibility requirement often encountered in watermarking and data hiding applications. Furthermore, we illustrate, through simulation, the ability of the proposed model to efficiently capture the salient features of the underlying image regardless of the wavelet filters being used.**

I. Introduction

It is generally believed that the performance of most current watermarking systems is not close enough to the fundamental limit on robust watermark embedding rates at which high perceptual image quality is maintained. To support real applications demanding high-capacity and robust watermarking, more sophisticated perceptual image models are required. Borrowing results from image coding and compression [1], [2], [4], a seemingly unrelated topic to watermarking, perceptual models have been derived to reach the optimality bound from perceptual watermarking systems. Ghouti and Bouridane [3] suggest the use of a JND profile for balanced multiwavelets. It is worth noting that the model, defined in [3], does not depend on a specific set of multifilters. Watson [1] defines perceptually-optimal quantization matrices for JPEG standard. Chou and Li [4] propose a JND profile for an optimal image subband coder. Watson et al. [2] define visibility thresholds of quantization noise for linear phase 9/7 wavelet filters. These models have been successfully used to achieve imperceptible watermark embedding [5]. Kundur and Hatzinakos [6] propose a model to classify salient regions in host images for watermark embedding. Lu et al. [7] employ JND in the wavelet domain to obtain transparent watermarks of maximum strength. Barni et al. [8] exploit the characteristics of the human visual system (HVS), as well as the masking effect, to estimate the proper watermark signal strength for carrying out watermark embedding through wavelet coefficient modulation. To improve the performance of spread-spectrum watermarking, Kutter and Winkler [9] propose a perceptual model that takes into account the contrast sensitivity and texture masking. The goal of this paper is to develop an efficient, yet simple, perceptual model based on a subband decomposition that is specifically adopted to watermark embedding using any scalar wavelet transform.

L. Ghouti and A. Bouridane are with the School of Computer Science, Queen's University of Belfast, Belfast BT7 1NN, UK. Email: {LGhouti01,A.Bouridane}@qub.ac.uk

II. A Perceptual Model For Scalar Wavelets

We will give a brief overview of Ghouti's model and show its relevance to the scalar wavelet transforms [1] through the use of subbands' modeling. Ghouti and Bouridane [3] propose a JND or minimally noticeable distortion (MND) profile to quantify the "*perceptual redundancy*". The JND profile provides a visibility threshold of distortion for each image being analyzed. The latter indicates the level below which distortions due to watermark embedding are rendered imperceptible. The JND profile incorporates two major factors, known to be influential in the human visual perception; namely the "*background luminance*" and "*texture masking effect*". The purpose of the JND profile is to guide the watermark embedding in the wavelet domain [5]. Therefore, this profile must be decomposed into component JND/MND profiles of different frequency/orientation subbands. With the decomposed profile, watermark data will be adaptively embedded into subband coefficients according to their "*perceptual significance*".

A. Perceptual Redundancies

The imperfections and the inconsistency in sensitivity inherent to the human visual system (HVS) allow for "*perceptual redundancies*". Psychovision studies [10] indicate that the visibility threshold of a particular stimulus depends on many factors. There are primarily two major factors that affect the error visibility threshold of each pixel [2]. These two factors are:

- Luminance Contrast: Human visual perception is sensitive to luminance contrast rather than absolute luminance value. As indicate by Weber's law, if the luminance of a test stimulus is just noticeable from the surrounding luminance, then the ratio of just noticeable luminance difference to stimulus difference, known as *Weber fraction*, is constant.
- Spatial Masking: The second factor reflects the fact that the reduction in the visibility of the stimuli is caused

[1]One of the major merits of this model is its independence of the wavelet kernels unlike the model proposed in [2]. Therefore, this model will be valid for any multiresolution-based watermarking system regardless of the transform kernels being used.

[2]Only achromatic images in the spatial domain are considered. Hence, the JND/MND profile must be decomposed to fit a subband decomposition structure.

by the increase in the spatial nonuniformity of the background luminance. This fact is known as *spatial masking*.

Following the work of [4], the perceptual model of [3] estimates, from pixels in the spatial domain, the JND value associated with each pixel in the image. Strictly speaking, the visibility threshold of JND is a very complex process and depends on the afore-mentioned factors. However, in [3], [4] the inter-relevance of the two factors is simplified and the JND value is defined as the dominant effect of the two factors. The perceptual model for estimating the "*full-band JND*" profile is described by the following expressions [3], [4]:

$$JND_{fb}(x,y) = \max\{f_1(b_g(x,y), m_g(x,y)), f_2(b_g(x,y))\} \quad (1)$$

$$f_1(b_g(x,y), m_g(x,y)) = m_g(x,y)\alpha(b_g(x,y)) + \beta(b_g(x,y)) \quad (2)$$

$$f_2(b_g(x,y)) = \begin{cases} T_0 \cdot \left(1 - \left(\frac{b_g(x,y)}{127}\right)^{1/2}\right) + 3 \\ \quad \text{for } b_g(x,y) \le 127 \\ \gamma \cdot (b_g(x,y) - 127) + 3 \\ \quad \text{for } b_g(x,y) > 127 \end{cases} \quad (3)$$

$$\alpha(b_g(x,y)) = b_g(x,y) \cdot 0.0001 + 0.115 \quad (4)$$

$$\beta(b_g(x,y)) = \lambda - b_g(x,y) \cdot 0.001 \quad (5)$$

where $b_g(x,y)$ and $m_g(x,y)$ are the average background luminance and the maximum weighted average luminance differences around the pixel at (x,y), respectively. The spatial masking effect is taken into account by the function $f_1(x,y)$, the linear behavior of which is obtained from psychovisual tests [4]. The visibility threshold due to background luminance is given by the function $f_2(x,y)$ in which the relationship between noise sensitivity and the background luminance is verified by a subjective test [4]. The parameters $\alpha(x,y)$ and $\beta(x,y)$ are background-dependent functions derived through psychovisual experiments. T_0 and γ denote, respectively, the visibility threshold when the background grey level is 0, and the slope of the linear function relating the background luminance to visibility threshold at higher background luminance (level higher than 127). Parameter λ affects the average amplitude of visibility threshold due to spatial masking effect. During the conducted experiments in [4], T_0, γ, and λ are found to be 17, $\frac{3}{128}$, and $\frac{1}{2}$, respectively.

B. Deriving MND Profile

To accommodate different embedding strengths, the MND profile of different distortion levels are required. In this case, the MND profile is obtained by simply multiplying every element of the JND profile, defined in (1), by a constant scale factor d as a distortion index. Thus, the MND profile with a distortion index, d, can be expressed as [3], [4]:

$$MND_{d,fb}(x,y) = JND_{fb}(x,y) \cdot d \quad (6)$$

where the value of d ranges from 1.0 to 4.0. The $m_g(x,y)$ across the pixel at (x,y) is determined by calculating the weight average of luminance changes around the pixel in four directions. Four operators $G_k(i,j)$ for $i,j = 1,2,\ldots,5$, are employed to perform the calculations, where the weighting coefficient decreases as the distance away from the central pixel increases. The weight operators, G_k are given by [3], [4]:

$$G_1 = \begin{bmatrix} 0 & 0 & 0 & 0 & 0 \\ 1 & 3 & 8 & 3 & 1 \\ 0 & 0 & 0 & 0 & 0 \\ -1 & -3 & -8 & -3 & -1 \\ 0 & 0 & 0 & 0 & 0 \end{bmatrix} \quad G_2 = \begin{bmatrix} 0 & 0 & 1 & 0 & 0 \\ 0 & 8 & 3 & 0 & 0 \\ 1 & 3 & 8 & -3 & -1 \\ 0 & 0 & -3 & -8 & 0 \\ 0 & 0 & -1 & 0 & 0 \end{bmatrix}$$

$$G_3 = \begin{bmatrix} 0 & 0 & 1 & 0 & 0 \\ 0 & 0 & 3 & 8 & 0 \\ -1 & -3 & 0 & 3 & 1 \\ 0 & -8 & -3 & 0 & 0 \\ 0 & 0 & -1 & 0 & 0 \end{bmatrix} \quad G_4 = \begin{bmatrix} 0 & 1 & 0 & -1 & 0 \\ 0 & 3 & 0 & -3 & 0 \\ 0 & 8 & 0 & -8 & 0 \\ 0 & 3 & 0 & -3 & 0 \\ 0 & 1 & 0 & -1 & 0 \end{bmatrix} \quad (7)$$

Using the weights defined in (7), the maximum weighted average of luminance differences, $m_g(x,y)$, is given by the following expression:

$$m_g(x,y) = \max_{k=1,2,3,4}\{|grad_k(x,y)|\} \quad (8)$$

where

$$|grad_k(x,y)| = \frac{1}{16}\sum_{i=1}^{5}\sum_{j=1}^{5} p(x-3+i, y-3+j) \cdot G_k(i,j) \quad (9)$$

where $p(x,y)$ denotes the pixel at position (x,y). The average background luminance , $b_g(x,y)$, is calculated by a weighted operator, $B(i,j), i,j = 1,2,\ldots,5$.

$$b_g(x,y) = \frac{1}{32}\sum_{i=1}^{5}\sum_{j=1}^{5} p(x-3+i, y-3+j) \cdot B(i,j) \quad (10)$$

where the weight factor, $B(i,j)$ is given by:

$$B(i,j) = \begin{bmatrix} 1 & 1 & 1 & 1 & 1 \\ 1 & 2 & 2 & 2 & 1 \\ 1 & 2 & 0 & 2 & 1 \\ 1 & 2 & 2 & 2 & 1 \\ 1 & 1 & 1 & 1 & 1 \end{bmatrix} \quad (11)$$

C. Decomposition of the JND/MND Profile

Since Chou's perceptual model does not address watermarking applications, the JND/MND profile must be modified to accommodate the decomposition structure obtained using scalar wavelet transforms. For an $N \times N$ image, the JND/MND profile, as originally proposed by [4], has the linear subband structure shown in Fig. 1.

As suggested by the HVS models and human perception sensitivity, the high frequency subbands have higher weights. However, the linear decomposition structure, shown in Fig. 1, does not lend itself to such a property. Therefore, we

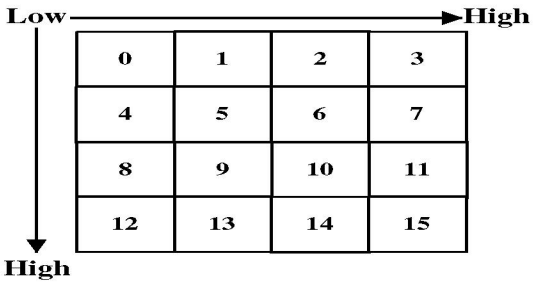

Fig. 1. Subband decomposition structure.

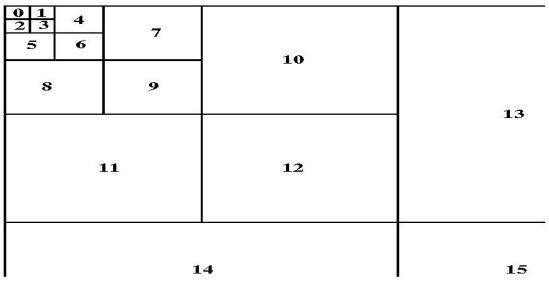

Fig. 2. JND profile structure for wavelet subbands using five decomposition levels.

need to find a suitable decomposition according to the frequency content of the wavelet subbands. Such a solution is presented in Fig. 2. Using the multiresolution decomposition and the modified JND profile, Figs. 3-4 show the resulting JND/MND profiles, based on linear phase 9/7 filters, for Lena and Barbara images, respectively. These figures clearly show the ability of the proposed JND/MND profile to adaptively adjust itself to the image activity. Therefore, edges and salient features are efficiently discriminated as highlighted in Figs. 3-4. This property is a key factor to satisfy the imperceptibility requirement often encountered in watermarking applications [5]. Furthermore, to illustrate the universality of the proposed model and its independence from the transform kernels, Fig. 5 shows the resulting JND/MND profiles, based on orthogonal Daubechies (Daub8) wavelets, for Lena and Barbara images, respectively. From a comparison between Figs. 3-4 and Fig. 5, it is clear that the proposed model yields "*virtually*" similar profiles for different wavelet kernels. Finally, Fig. 6 illustrates the resulting JND/MND profile for Lena image based on balanced multiwavelets.

Finally, the JND/MND profile should be decomposed to fit the subband structure shown in Fig. 2. The subband profile is given by:

$$JND_q^2(x,y) = \left[\sum_{i=0}^{3}\sum_{j=0}^{3} JND_{fb}^2(i+x\cdot 4, j+y\cdot 4)\right]\cdot\omega_q$$
$$\text{for } q=0,1,\cdots,15, \text{ and } 0\le x\le \tfrac{N}{4},\ \ 0\le y\le \tfrac{N}{4}$$

where $JND_q(x,y)$ denotes the magnitude of the JND at position (x,y) of the q^{th} subband (see Fig. 2). The factor ω_q, representing the q^{th} subband weight, is defined by the following expression:

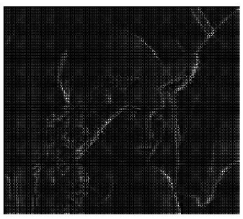

Fig. 3. Lena image (left) and its resulting JND/MND profile (right) based on 9/7 linear phase filters.

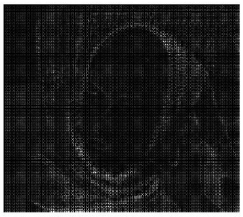

Fig. 4. Barbara image (left) and its resulting JND/MND profile (right) based on 9/7 linear phase filters.

$$\omega_q = \left(S_q\cdot\sum_{k=0}^{15} S_k^{-1}\right)^{-1},\quad \text{for } q=0,1,\cdots,15, \tag{12}$$

where S_k denotes the average sensitivity of the HVS to spatial frequencies in the kth subband. The average sensitivity, S_k, is given by [4]:

$$S_k = \frac{16}{N\cdot N}\sum_{u=\epsilon_k\cdot h}^{(\epsilon_k+1)h-1}\ \sum_{v=\rho_k\cdot w}^{(\rho_k+1)w-1}\xi(u,v) \quad \text{for } k=0,1,\cdots,15, \tag{13}$$

where

$$h=\frac{N}{4},\quad w=\frac{N}{4},\quad \epsilon_k=\lfloor\frac{k}{4}\rfloor,\quad \rho_k=k-\epsilon_k\cdot 4$$

and $\xi(u,v)$ denotes the response curve of the modulation transfer function (MTF) for $0\le u\le N$, $0\le v\le N$. Chou and Li [4] propose the following generalized formula for fitting the response curve of the MTF:

$$\xi(u,v)=a\cdot\left[b+\left(\frac{\Omega(u,v)}{\Omega_0}\right)\right]\cdot\exp\left[-\left(\frac{\Omega(u,v)}{\Omega_0}\right)^c\right] \tag{14}$$

where

$$\Omega(u,v) = \left[\left(\tfrac{32v}{N}\right)^2+\left(\tfrac{24u}{N}\right)^2\right]^{\frac{1}{2}} \quad \text{for } 0\le u\le N-1,\quad 0\le v\le N-1 \tag{15}$$

is the spatial frequency in cycles per degree (cpd) and Ω_0 is a shaping parameter for the MTF curve [4]. It should be noted that the JND profiles shown in Figs. 3-4 are derived for the MTF curve modeled by $a=2.6$, $b=0.0192$, $c=1.1$, $\Omega_0=8.772$, $T_0=17$, $\gamma=\frac{3}{128}$, and $\lambda=\frac{1}{2}$, respectively. The distortion index, d, is fixed to 3.0. The subband JND profile subbands, $JND_q(x,y)$, are inverse-transformed to obtain the spatial JND profiles shown in Figs. 3-6.


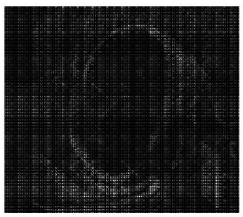

Fig. 5. JND/MND profile for Lena image (left) and JND/MND profile for Barbara image (left) based on orthogonal Daub8 wavelets.


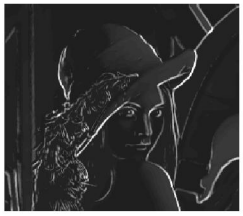

Fig. 6. Lena image (left) and its resulting JND/MND profile (right) based on balanced multiwavelets.

III. Perceptual Image Watermarking Using JND Profiles of Scalar Wavelets

Using the perceptual model proposed in Section II, we implement the perceptual watermarking system introduced in [3]. The watermarking system has the following embedding rule used:

$$x_j = s_j \left(1 + \alpha_j p n_j m_k\right), j = 1, 2 \ldots, \chi \tag{16}$$

where,

- s_j represents the host transform coefficient selected from a set to hide the watermark bit m_k. Each watermark bit, $m_k, 1 \leq k \leq M$, is embedded in a set containing χ host transform coefficients. $m_k \pm 1$.
- x_j is the watermarked transform coefficient.
- α_j is the JND profile weight (variable) calculated based on the perceptual model described in Section II.
- pn_j is the pseudo-random coefficient used to modulate the watermark bit m_k.

For illustration purposes, we present results of the performance of the proposed system where we assume no attacks against the embedded watermarks. The embedded watermark messages consist of 128, 256, 512, and 1024 bits, respectively. Fig. 7 shows the bit error rate (BER) of the JND-based perceptual watermarking system. In Fig. 8, we show results for the performance of the decoder in the presence of AWGN noise. The watermark messages consist of 256 bits.

IV. Conclusions

In this paper, we have proposed a novel perceptual model for scalar wavelets based on JND profiles derived using HVS models. Unlike the existing perceptual models, the proposed one is independent of the transform kernels being used. Finally, to illustrate the performance of the perceptual model, we integrated this model into a spread-spectrum image watermarking system to account for imperceptibility requirements often encountered in watermarking applications.

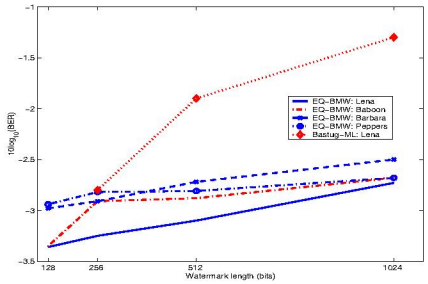

Fig. 7. Logarithmic BERs of repetition-coding using BMW method and block DCT for various watermark lengths ($M = 128, 256, 512$, and 1024).

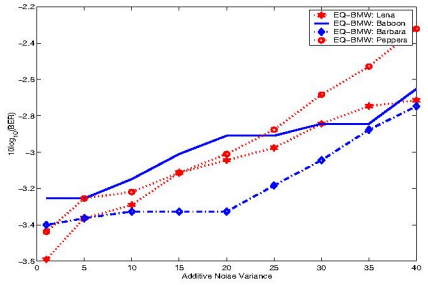

Fig. 8. Logarithmic BERs of BCH (15, 7) code in the presence of AWGN noise using watermark length of 256 bits.

V. Acknowledgment

The authors would like to thank Dr. A. Ahumada (NASA Ames Research Center, USA) and Prof. D. Pelli (New York University, USA) for their willingness to answer our questions on psychovision.

References

[1] A. B. Watson, "Perceptual optimization of DCT color quantization matrices," *IEEE Int. Conf. Image Processing*, vol. 1, pp. 100-104, Nov. 1994.

[2] A. B. Watson and G. Yang and J. Solomon and J. Villasenor, "Visibility of wavelet quantization noise," *IEEE Trans. Image Processing*, vol. 6, no. 8, pp. 1164-1175, Aug. 1997.

[3] L. Ghouti and A. Bouridane , "A Just-Noticeable Distortion (JND) Profile for Balanced Multiwavelets," in *European Signal Processing Conference*, (EUSIPCO 2005), Antalya, Turkey, Sept. 2005.

[4] C-H. Chou and Y-C. Li, "A perceptually tuned subband image coder based on the measure of just-noticeable distortion profile," *IEEE Trans. Circuits and Systems for Video Technology*, vol. 5, no. 6, pp. 467-476, Dec. 1995.

[5] C. I. Podilchuk and W. Zeng, "Image-adaptive watermarking using visual models," *IEEE J. on Select. Areas Commun.*, vol. 16, no. 4, pp. 525-539, May 1998.

[6] D. Kundur and D. Hatzinakos, "Towards robust logo watermarking using multiresolution image fusion principles," *IEEE Trans. Multimedia*, vol. 6, no. 1, pp. 185-198, Feb. 2004.

[7] C-S. Lu, S-K. Huang, C-J. Sze, and H-Y. M. Lino, "Cocktail watemarking far digital image protection," *IEEE Trans. Multimedia*, vol. 2, no. 4, pp. 209-224, Dec. 2000.

[8] M. Barni, F. Bartolini, and A. Piva, "Improved wavelet-based watermarking through pixel-wise masking," *IEEE Trans. Image Processing*, vol. 10, no. 5, pp. 783-791, May. 2001.

[9] M. Kutter and S. Winkler, "A vision-based masking model for spread-spectrum image watermarking," *IEEE Trans. Image Processing*, vol. 11, no. 1, pp.16-25, Jan 2002.

[10] K. H. Zou, T. R. Hsing and J. G. Dunham, "Applications of physiological human visual system model to image compression," in *Proc. SPIE*, vol. 504, pp. 419-424, 1984.